Mechanics of the Segmentation of an Embedded Fiber, Part II: Computational Modeling and Comparisons

A. P. S. Selvadurai
Department of Civil Engineering and Applied Mechanics,
Faculty of Engineering,
McGill University,
Montreal, QC H3A 2K6, Canada
Mem. ASME

A. ten Busschen
Laboratory of Engineering Mechanics,
Faculty of Mechanical Engineering and Marine Technology,
Delft University of Technology,
Delft, The Netherlands

A fragmentation test has been developed for the study of the influence of the adhesive characteristics of the interface between reinforcing fibers and the matrix on the development of matrix cracking at a cracked single fiber location. The present paper examines the numerical modeling of the crack extension process within the matrix region. The numerical modeling focuses on the application of boundary element techniques to the study of an axisymmetric fiber-matrix model and quasi-static crack extension criteria are employed to determine the path of crack extension. The result for the crack extension patterns obtained from the numerical models are compared with the results derived from the experiments. It is shown that elastic fracture mechanics simulations of quasi-static crack extension can successfully model the observed experimental phenomena.

Introduction

The integrity of bond between a fiber and the surrounding matrix is of fundamental importance to the successful development and adaptation of fiber-reinforced composite materials. The interface bond characteristics are important from the point of view of both longitudinal and transverse resistance to fracture and failure of fiber-reinforced composites. Debonding, delamination, and cracking at a fiber-matrix interface can be initiated by a variety of factors including stress concentrations at sharp edges, inhomogeneities, thermal mismatch between the matrix, and the reinforcement and other environmentally induced loading effects. The evaluation of the influence of such defects on fracture propagation, stiffness degradation, etc., can significantly enhance both performance evaluation and material selection for fiber-reinforced composites (Sih and Tamuzs, 1979; Selvadurai, 1981; Hashin and Herakovich, 1983; Kelly and Rabotnov, 1983; and Dvorak, 1991).

The companion paper (Busschen and Selvadurai, 1995) focussed on the experimental evaluation of the influence of interface strength characteristics on the development of matrix cracking at a cracked fiber location. The stress transfer between the fiber and the matrix and vice versa, is achieved by means of a bonding mechanism (i.e., chemical bonding and mechanical interlock) or by means of a slip mechanism (friction between matrix and crack). These two mechanisms can be characterized experimentally for a specific fiber-matrix combination. A well-known test used for this purpose is a "pull-out" test (Piggott, 1980), which consists of a single fiber which is embedded in a matrix. This method of fiber-matrix interface characterization is, however, both time-consuming and highly sensitive to the test procedure. This research program advocates the development and use of the fragmentation test which provides information about the role of the interface strength characteristics on the subsequent development of matrix fracture. The testing of a composite specimen, in which a single fiber is embedded within a larger matrix region, permits not only ease of testing but also a clearer study of extended matrix fracture generation at a cracked fiber location. The companion paper has characterized the morphology of matrix crack patterns which can exist in a fragmentation test particularly in the presence of strong interface bonding, i.e., the interface strength and fracture toughness characteristics are expected to be much larger than the corresponding properties for the matrix region.

The primary objective of this paper is to examine whether the fracture morphologies observed in the fragmentation tests can be predicted by appeal to current developments in fracture mechanics. It must be observed that fracture morphology is one of the main observations of the fragmentation test. Due to the relatively small area of the fiber cross-section its influence on the overall load-displacement behavior of the

Contributed by the Applied Mechanics Division of THE AMERICAN SOCIETY OF MECHANICAL ENGINEERS for publication in the ASME JOURNAL OF APPLIED MECHANICS.

Discussion on this paper should be addressed to the Technical Editor, Professor Lewis T. Wheeler, Department of Mechanical Engineering, University of Houston, Houston, TX 77204-4792, and will be accepted until four months after final publication of the paper itself in the ASME JOURNAL OF APPLIED MECHANICS.

Manuscript received by the ASME Applied Mechanics Division, Dec. 2, 1992; final revision, Oct. 8, 1993. Associate Technical Editor: G. J. Dvorak.

fragmentation specimen is not significant. Attention is therefore focussed on a numerical modeling scheme which will examine the quasi-static crack extension within the matrix in the presence of strong adhesion.

The numerical modeling of fracture can be approached by adopting either finite element techniques or boundary element techniques. Accounts of these developments together with extensive references to developments in these areas are given by Zienkiewicz (1977), Brebbia et al. (1984), Brebbia and Aliabadi (1991), and Atluri (1991). In this paper, the boundary element technique is used to study the evolution of quasi-static crack extension into the matrix region at a cracked fiber location.

The Boundary Element Method

The formulation of the boundary element method for elastostatic problems is given by Banerjee and Butterfield (1981) and Brebbia et al. (1984). In this section a brief exposition of the basic features of the method are summarized for completeness. Further details of the application of boundary element techniques to the computational modeling of problems in fracture mechanics are given by Cruse and Wilson (1977), Blandford et al. (1981), Smith and Mason (1982), and Selvadurai and Au (1986, 1988, 1989, 1991).

We specifically consider the problem of a cylindrical elastic fiber which is embedded in bonded contact with an elastic matrix region of infinite extent. We assume that the fiber develops a plane crack normal to its axis due to the application of a uniform axial strain to the entire composite region. As indicated previously (Busschen and Selvadurai, 1995), the further application of uniform straining will induce either matrix cracking or fiber-matrix interface delamination. In the numerical modeling we primarily focus attention on the matrix cracking problem which persists in the presence of strong interface adhesion. The three main modes of matrix cracking include the following: (i) the development of a penny-shaped crack, (ii) the development of a conoidal crack, or (iii) the development of a combined conoidal crack-penny-shaped crack, at the cracked fiber location. As observed in the experiments, three-dimensional helicoidal cracks can occur in the fragmentation tests; these, however, do not abound. The boundary element technique in conjunction with crack extension criteria are used to establish the computational predictions for crack extension. Admittedly, the fracture propagation in a brittle material such as the matrix of a fiber-reinforced structural element is usually a dynamic phenomenon. In the fragmentation test, however, it is observed that the growth of the fracture in the matrix region can be effectively controlled to minimize dynamic aspects of crack extension. For this reason, the boundary element modeling is restricted only to the static problem.

We assume that both the uniform straining of the fragmentation test specimen and the resulting extension of matrix cracking exhibit a state of symmetry about the axis of the embedded fiber (Fig. 1). Both the fiber and matrix regions are assumed to be isotropic elastic materials which satisfy the stress-strain relationship

$$\sigma_{ij}^{(\alpha)} = \lambda_\alpha \delta_{ij} u_{k,k}^{(\alpha)} + G_\alpha \left\{ u_{ij}^{(\alpha)} + u_{j,i}^{(\alpha)} \right\} \tag{1}$$

and the Navier equations

$$G_\alpha \nabla^2 u_i^{(\alpha)} + (\lambda_\alpha + G_\alpha) u_{k,ki}^{(\alpha)} = 0 \tag{2}$$

where G_α and λ_α are Lame's constants; the subscript or superscript "α" refers to the matrix (m) and fiber (f) regions; u_i and σ_{ij} are, respectively, the displacement components and stress tensor referred to the rectangular Cartesian coordinate system x, y, z; i, $j = x$, y, z; $\lambda_\alpha = 2G_\alpha \nu_\alpha/(1 - 2\nu_\alpha)$; ν_α are Poisson's ratios; $G_\alpha = E_\alpha/2(1 + \nu_\alpha)$; ∇^2 is

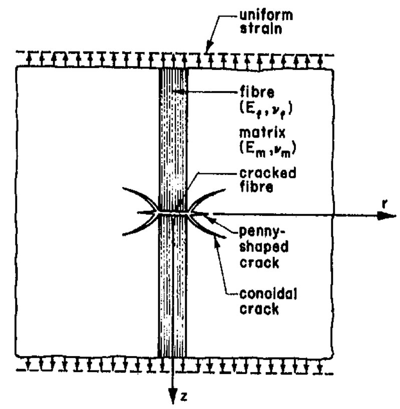

Fig. 1 The axisymmetric model of the fragmentation tests for an embedded fiber

Laplace's operator referred to the rectangular Cartesian coordinate system; and δ_{ij} is Kronecker's delta function. Here, and in what follows, the Greek indices and subscripts will refer to quantities pertaining to the matrix and fiber regions.

The boundary integral equation for the axisymmetric problem pertaining to the fiber-matrix composite region can be written in the form (see, e.g., Kermanidis, 1975; Cruse and Wilson, 1977)

$$c_{\ell k} u_k^{(\alpha)} + \int_{\Gamma_\alpha} \left\{ P_{\ell k}^{*(\alpha)} u_k^{(\alpha)} - u_{\ell k}^{*(\alpha)} P_k^{(\alpha)} \right\} \frac{r}{r_i} d\Gamma = 0 \tag{3}$$

where Γ_α is the boundary of the region α; $u_k^{(\alpha)}$ and $P_k^{(\alpha)}$ are, respectively, the displacements and tractions on the boundary Γ_α and $u_{ik}^{*(\alpha)}$ and $P_{ik}^{*(\alpha)}$ are fundamental solutions. Also in (3), c_{ij} is a constant ($= 0$, if the point is outside the body; $= \delta_{ij}$ if the point is inside the body; $= \delta_{ij}/2$ if the point is located at a smooth boundary, and is a function of discontinuity at a corner and of Poisson's ratio (Banerjee and Butterfield, 1981)).

For axial symmetry

$$u_{rr}^{*(\alpha)} = C_1 \left\{ \frac{4(1-\nu_\alpha)(\rho^2 + \bar{z}^2) - \rho^2}{2r\bar{R}} \right\} K(\bar{m}) - \left\{ \frac{(7 - 8\nu_\alpha)}{4r} \bar{R} - \frac{(e^4 - \bar{z}^4)}{4r\bar{R}^3 m_1} \right\} E(\bar{m}) \tag{4}$$

$$u_{rz}^{*(\alpha)} = C_1 \bar{z} \left[\frac{(e^2 + \bar{z}^2)}{2\bar{R}^3 m_1} E(\bar{m}) - \frac{1}{2\bar{R}} K(\bar{m}) \right] \tag{5}$$

$$u_{zr}^{*(\alpha)} = C_1 r_i \bar{z} \left[\frac{(e^2 - \bar{z}^2)}{2r\bar{R}^3 m_1} E(\bar{m}) + \frac{1}{2r\bar{R}} K(\bar{m}) \right] \tag{6}$$

$$u_{zz}^{*(\alpha)} = C_1 r_i \left[\frac{(3 - 4\nu_\alpha)}{\bar{R}} K(\bar{m}) + \frac{\bar{z}^2}{\bar{R}^3 m_1} E(\bar{m}) \right] \tag{7}$$

where

$$\bar{z} = (z - z_i); \quad \bar{r} = (r + r_i); \quad \rho^2 = (r^2 + r_i^2)$$

$$e^2 = (r^2 - r_i^2); \quad \bar{R}^2 = \bar{r}^2 + \bar{z}^2; \quad C_1 = \frac{1}{4\pi G_\alpha (1 - \nu_\alpha)}$$

$$\bar{m} = \frac{2rr_i}{\bar{R}^2}; \quad m_1 = 1 - \bar{m} \tag{8}$$

and $K(\bar{m})$ and $E(\bar{m})$ represent, respectively, the complete elliptic integrals of the first and second kind. The corresponding terms for the traction fundamental solution $P^{*(\alpha)}_{\ell k}$ can be obtained by the manipulation of the results (4) to (7).

Upon discretization of the boundaries Γ_α into boundary elements, the integral Eq. (3) can be represented in the form of a boundary element matrix equation as follows:

$$\left[\mathbf{H}^{(\alpha)}\ \mathbf{H}_I^{(\alpha)}\right]\begin{bmatrix}\mathbf{u}^{(\alpha)}\\ \mathbf{u}_I^{(\alpha)}\end{bmatrix} = \left[\mathbf{M}^{(\alpha)}\ \mathbf{M}_I^{(\alpha)}\right]\left[\mathbf{P}^{(\alpha)}\ \mathbf{P}_I^{(\alpha)}\right] \quad (9)$$

where **H**'s and **M**'s are the influence coefficient matrices derived from the integration of the fundamental solutions $P^{*(\alpha)}_{\ell k}$ and $u^{*(\alpha)}_{\ell k}$, respectively. In the instance where there is complete bonding between the fiber-matrix interface we have

$$\mathbf{u}_I^{(f)} = \mathbf{u}_I^{(m)} = \mathbf{u}_I$$
$$\mathbf{P}_I^{(f)} = -\mathbf{P}_I^{(m)} = \mathbf{P}_I. \quad (10)$$

Using the above result, the complete matrix equation governing the fiber composite-crack interaction problem can be expressed in the form

$$\begin{bmatrix}\mathbf{H}^{(f)} & \mathbf{H}_I^{(f)} & 0\\ 0 & \mathbf{H}_I^{(m)} & \mathbf{H}^{(m)}\end{bmatrix}\begin{bmatrix}\mathbf{u}^{(f)}\\ \mathbf{u}_I\\ \mathbf{u}^{(m)}\end{bmatrix} = \begin{bmatrix}\mathbf{M}^{(f)} & \mathbf{M}_I^{(f)} & 0\\ 0 & \mathbf{M}_I^{(m)} & \mathbf{M}^{(m)}\end{bmatrix}\begin{bmatrix}\mathbf{P}^{(f)}\\ \mathbf{P}_I\\ \mathbf{P}^{(m)}\end{bmatrix}. \quad (11)$$

Modeling of Crack-Tip Behavior

In the boundary element discretizations discussed in the previous section, quadratic elements will be employed to model the boundaries of the matrix and fiber regions. That is, the variation of the displacements and tractions within an element can be described by

$$\left.\begin{matrix}u_i^{(\alpha)}\\ P_i^{(\alpha)}\end{matrix}\right\} = a_0 + a_1\zeta + a_2\zeta^2 \quad (12)$$

where ζ is the local coordinate of the element and a_r ($r = 0$, 1, 2) are constants of interpolation. However, in the context of linear elastic fracture mechanics, the stress field at the crack tip should contribute to a $1/\sqrt{r}$-type singularity. In the finite element technique, the quarter-point element of the type proposed by Henshell and Shaw (1975) and Barsoum (1976) can be used to model the required $\sqrt{r}$-type variation of the displacements. That is, if the same type of element is implemented in a boundary element method where b_i ($i = 0$, 1, 2) are constants

$$\left.\begin{matrix}u_i^{(\alpha)}\\ P_i^{(\alpha)}\end{matrix}\right\} = b_0 + b_1\sqrt{r} + b_2 r. \quad (13)$$

Since the $P_i^{(\alpha)}$ in (13) does not produce a $1/\sqrt{r}$-type singularity, Cruse and Wilson (1977) developed the so-called "singular traction quarter-point boundary element," where the traction variations in (13) are multiplied by a nondimensional $\sqrt{\ell/r}$ where ℓ is the length of the crack-tip element. The variations of tractions can be expressed in the form

$$P_i = \frac{c_0}{\sqrt{r}} + c_1 + c_2\sqrt{r} \quad (14)$$

where c_i ($i = 0, 1, 2$) are constants. The performance of both types of quarter-point elements have been studied by Blandford et al. (1981), Smith and Mason (1982), and Selvadurai and Au (1989) and their accuracy established by comparison with known exact solutions.

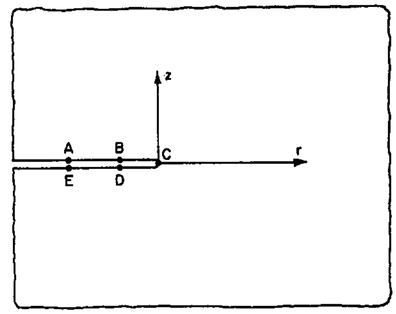

Fig. 2 Detail at the crack tip. Node arrangement for the computation of the stress intensity factor.

In the crack-fiber interaction problem examined in this paper the axial straining induces a state of axial symmetry in the fiber-matrix composite region. Consequently, only the Mode I and Mode II stress intensity factors are present at the tips of the crack region. The flaw opening-mode stress intensity factor can be evaluated by applying the displacement correlation method which utilizes the nodal displacements at four locations A, B, E, D, and the crack tip (Fig. 2) i.e.,

$$K_I^{(\alpha)} = \frac{G_\alpha}{(k_\alpha + 1)}\sqrt{\frac{2\pi}{\ell_0}}\left\{4[u_z(B) - u_z(D)] + u_z(E) - u_z(A)\right\} \quad (15)$$

where $k_\alpha = (3 - 4\nu_\alpha)$ and ℓ_0 is the length of the crack-tip element. Similarly the flaw shearing mode stress intensity factor can be written in the form

$$K_{II}^{(\alpha)} = \frac{G_\alpha}{(k_\alpha + 1)}\sqrt{\frac{2\pi}{\ell_0}}\left\{4[u_r(B) - u_r(D)] + u_r(E) - u_r(A)\right\}. \quad (16)$$

Crack Extension Criteria

The boundary element technique described in the previous section can be applied to examine the mechanics of matrix crack extension at the cracked fiber location. In order to develop the computational model it is necessary to establish a crack extension criterion applicable to the brittle matrix region. The subject of fracture extension in brittle elastic solids has been studied very extensively over the past two decades. Such studies have been motivated by the interest in the examination of crack extension in both metallic materials such as steel and nonmetallic materials such as concrete, rock, ceramic materials, polymeric materials at low temperatures, and ice. Extensive accounts of these developments can be found in the literature on fracture mechanics (see, e.g., Liebowitz, 1968; Kassir and Sih, 1975; Atkinson, 1979; Cherepanov, 1979; Lawn and Wilshaw, 1980; Broek, 1982; Kanninen and Popelar, 1985; Shaw and Swartz, 1987; Sih, 1991). In studies related to crack extension in brittle elastic solids, it is necessary to postulate two criteria. The crack extension criterion establishes the stress conditions necessary for the onset of crack extension. The second relates to the criterion which establishes the orientation of crack growth.

(a) Criteria for Onset of Crack Extension. The onset of crack extension in brittle elastic solids can be described by a variety of criteria. Such criteria are invariably developed on the basis of experimental investigations on fracture toughness testing of materials such as concrete mortar, rock, and brittle ceramics. A simple form of a criterion for the onset of crack extension can be expressed in terms of the fracture toughness

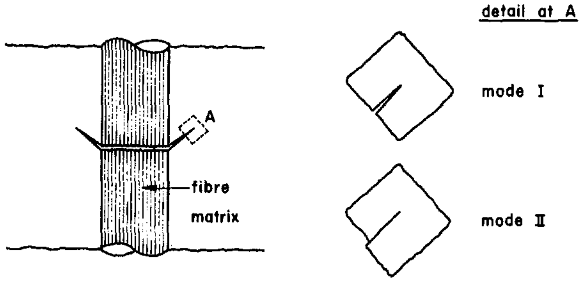

Fig. 3 Fracture modes at tip of matrix crack

of the material in the crack-opening mode. Accordingly, crack extension can be initiated when

$$K_I = K_{Ic} \tag{17}$$

where K_{Ic} is the critical value of the stress intensity factor in the crack-opening mode.

The result (17) can be generalized to include the influence of mode II or flaw shearing effects. The simplest form of a generalization due to Hellan (1985) takes the form

$$a_1\left(\frac{K_I}{K_{Ic}}\right)^2 + a_2\left(\frac{K_I}{K_{Ic}}\right) + a_3\left(\frac{K_{II}}{K_{IIc}}\right)^2 + a_4\left(\frac{K_{II}}{K_{IIc}}\right) = a_1 + a_2 \tag{18}$$

where K_{IIc} is the critical value of the stress intensity factor in the flaw shearing mode and a_i $(i = 1, 2, 3, 4)$ are experimentally derived constants.

The studies by Sih (1974) indicate that a generalized theory for the onset of crack extension can be posed in relation to the local strain energy density at the crack tip. The theory does not require the calculation of energy release rate and thus possesses the inherent advantage of being able to accommodate crack extension processes in which all modes of crack extension (in this case the Modes I and II) contribute to the local strain energy density function. The strain energy density function S at the crack boundary (Fig. 3) can be written as

$$S = \alpha_{11}K_I^2 + 2\alpha_{12}K_IK_{II} + \alpha_{22}K_{II}^2 \tag{19}$$

where

$$\alpha_{11} = \frac{1}{16G_m}(1 + \cos\theta)(\Omega - \cos\theta)$$

$$\alpha_{12} = \frac{1}{16G_m}\sin\theta[2\cos\theta(\Omega - 1)]$$

$$\alpha_{22} = \frac{1}{16G_m}[(\Omega + 1)(1 - \cos\theta) + (1 + \cos\theta)(3\cos\theta - 1)] \tag{20}$$

and

$$\Omega = \begin{cases} (3 - 4\nu_m) & \text{plane strain} \\ \dfrac{(3 - \nu_m)}{(1 + \nu_m)} & \text{plane stress} \end{cases} \tag{21}$$

depending upon whether the local stress field conforms either to a state of plane strain or plane stress. It can be shown that the stationary value of $S_{\min}$ can be used as an intrinsic material parameter the value of which at the onset of crack extension S_{cr} is independent of the crack geometry and loading.

(b) Orientation of Crack Growth. If we consider the conical elemental matrix crack with an arbitrary orientation to the cracked fiber location (Fig. 3), it is evident that at the crack-tip location both the stress intensity factors K_I and K_{II} are present. Consequently, a generalized crack extension criterion should incorporate the influence of both stress intensity factors. In this study the orientation of crack growth is examined by employing the criteria postulated by Erdogan and Sih (1963).

The maximum stress criterion assumes that the crack will start to extend in the plane which is normal to the maximum circumferential stress $\sigma_{\theta\theta}$ (i.e., stress state referred to the local polar coordinate system located at the crack tip) in accordance with the condition

$$K_I\sin\theta + K_{II}(3\cos\theta - 1) = 0 \tag{22}$$

for determining the initial angle of crack growth θ.

The criterion defined by (22) has been used quite extensively for the study of quasi-static crack extension paths in brittle elastic materials such as concrete, epoxy, ceramics, and rock. This is by no means the only available criterion which has been proposed for crack extension in mixed mode. References to such developments are given by Sih and Theocaris (1979) and Sih (1991).

Matrix Crack Development at the Cracked Fiber

First, the methodologies outlined in the previous sections are utilized to examine the crack extension into the matrix region at the cracked fiber location. In view of the application to the fragmentation test described by Busschen and Selvadurai (1995), attention is restricted to a typical E-glass fiber-polyester matrix system with the following basic properties.

E-Glass Fiber.

Diameter of fiber = 1.5×10^{-5} m = 15 μm
Elastic modulus of fiber = 70,000 MPa
Poisson's ratio of fiber = 0.20
Uniaxial tensile strength of fiber = 2500 MPa

Polyester Matrix.

Elastic modulus of matrix (E_m) = 1500 MPa
Poisson's ratio (ν_m) = 0.35
Uniaxial tensile strength (σ_T) = 87 MPa
Uniaxial compressive strength (σ_c) = 140 MPa
Critical stress intensity factor at seven days (K_{Ic}) = 1.0 MPa$\sqrt{m}$
Critical stress intensity factor post cure (K_{Ic}) = 0.6 MPa$\sqrt{m}$

The cross-sectional dimensions of the fragmentation test specimen in its midsection are 1 mm × 5 mm. When comparing the cross-sectional dimensions of the specimen with the diameter of the embedded fiber it is evident that the traction-free outer boundary of the specimen is located remote from the fiber (aspect ratio of 1/50). Consequently, in the numerical modeling attention is focussed on the problem of an elastic fiber which is embedded in an elastic matrix of infinite extent.

The primary objective of the exercise in numerical modeling is to use the concepts in crack extension discussed previously to predict the matrix crack patterns which originate at cracked fiber locations. It is assumed that at a cracked fiber location matrix cracking can originate in a variety of configurations. The origination of matrix cracking can be modeled as incremental starter cracks with basic conical or penny-shaped configurations which can occur either individually or simultaneously. The incremental penny-shaped starter cracks can

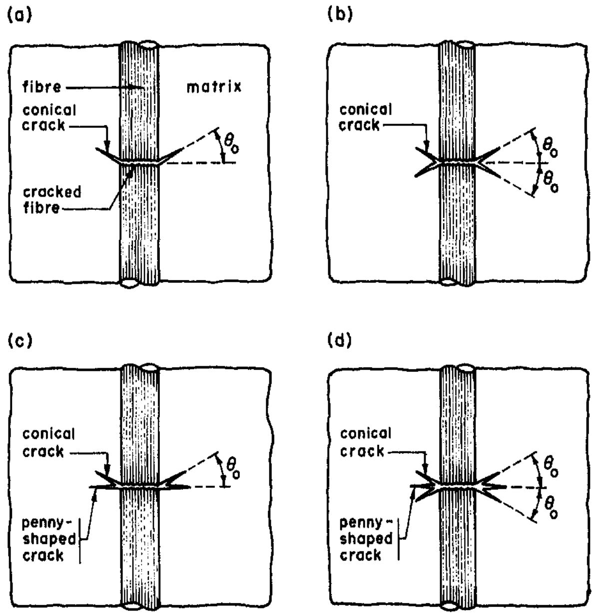

Fig. 4 Elemental matrix crack configurations at cracked fiber locations; (*a*) elemental conical crack, (*b*) elemental conical cracks which are symmetrically located about the plane of the cracked fiber, (*c*) a combination of an elemental penny-shaped crack and a single elemental conical crack, (*d*) a combination of an elemental penny-shaped crack and symmetrically placed elemental conical cracks, ($\theta_0 = \pi/2 - \varphi_0$)

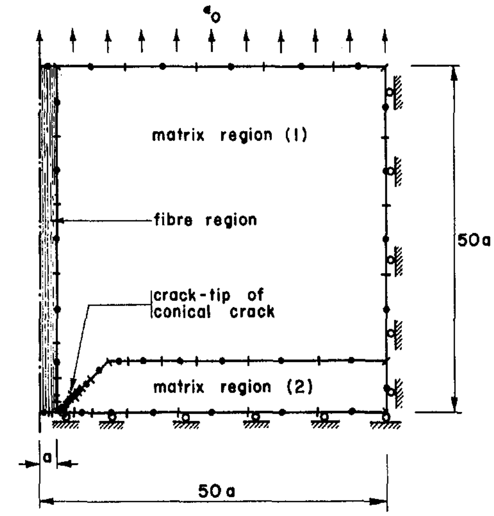

Fig. 5 Boundary element discretization used in the numerical modeling of the fragmentation test

occur in the plane of the cracked fiber and the incremental conical starter cracks are at an arbitrary orientation to the axis of the cracked fiber. Altogether four types of initial starter crack configurations can be examined. These include the following:

1 an elemental conical crack which is oriented at an arbitrary inclination to the fiber axis (Fig. 4(*a*)).
2 elemental conical cracks which are symmetrically located about the plane of the cracked fiber and oriented at an arbitrary inclination to the fiber axis (Fig. 4(*b*)).
3 a combination of an elemental penny-shaped crack and a single elemental conical crack which is oriented at an arbitrary inclination to the fiber axis (Fig. 4(*c*)).
4 a combination of an elemental penny-shaped cracked and symmetrically placed elemental conical cracks which are oriented at an arbitrary inclination to the fiber axis (Fig. 4(*d*)).

Admittedly, the scope of the numerical modeling can be extended to cover other conical elemental matrix crack configurations which are located nonsymmetrically with respect to the plane of the cracked fiber. The composite region containing the cracked fiber and the elemental cracks (Fig. 4) is subjected to a uniform far-field axial strain. A typical boundary element mesh discretization used in the numerical modeling of the fragmentation test is shown in Fig. 5. The extension of the crack and the path extension of the crack can be determined by considering the criteria for the onset of crack extension and the criteria for the orientation of incremental quasi-static crack growth.

In order to perform the numerical computations for the onset of crack extension by using the result (18) it is necessary to establish the critical values of the stress intensity factors governing both Mode I (K_{Ic}) and Mode II (K_{IIc}) fracture processes in the Polyester matrix. An examination of the literature on fracture toughness testing for the Polyester matrix material indicates that most such experimental evaluations of fracture toughness primarily focus on the determination of K_{Ic}. Further, for the Polyester matrix material, K_{IIc}, is expected to be much larger than the K_{Ic}. For this reason the criterion for the onset of crack extension is defined by the simpler criterion (17). This criterion has been very successfully adopted for the examination of fracture initiation in brittle solids such as concrete, rock, and ceramics.

With this *onset of crack extension criterion*, attention is focused on the specification of the orientation of crack growth. Preliminary investigations conducted by the authors on typical elemental starter crack configurations indicate that both criteria (22) and (24) give approximately the same results for the orientation of crack growth. The result of these studies cannot in any way be generalized. It is, however, convenient to adopt the simplified orientation of crack growth criterion defined by (22). With these simplified representations in mind, i.e., result (17) for the onset of crack extension and result (22) for the orientation of crack growth, the boundary element modeling procedure can be used to establish the quasi-static crack extension paths associated with the various starter crack configurations.

In the computations, the inclination of the conical starter crack to the axis of the fiber (θ_0) is set equal to 45 deg, 50 deg, 55 deg, and 60 deg. By assigning this range of conical starter crack orientations it is possible to assess their influence on the mode of crack extension. The lengths of the starter crack can be a variable; however, for the purposes of the numerical computations, the length of the starter crack (either conical or penny-shaped) is set equal to 0.01 a where a is the radius of the fiber.

We first consider the results developed for the case of an elemental conical crack which is located at an arbitrary orientation to the axis of the fiber. Figure 6 shows the crack extension pattern within the matrix region for starter crack orientation $\theta_0 \in$ (45 deg, 60 deg). The extent of matrix crack extension shown in Fig. 6 takes into consideration various levels of axial strain $\epsilon_0 \in (0.01, 0.12)$. In Fig. 7 we present the results for the strain-level-dependent crack extension patterns derived for the situation where conical starter cracks are symmetrically situated at the cracked fiber location. As is evident, either the symmetry or asymmetry in the orientation of the conical starter cracks appears to have a significant influence on the path of crack extension within the matrix.

We next consider the situation where both a penny-shaped starter crack and a nonsymmetric conical starter crack are present at the cracked fiber location. In this arrangement quasi-static crack extension can take place at either crack-tip

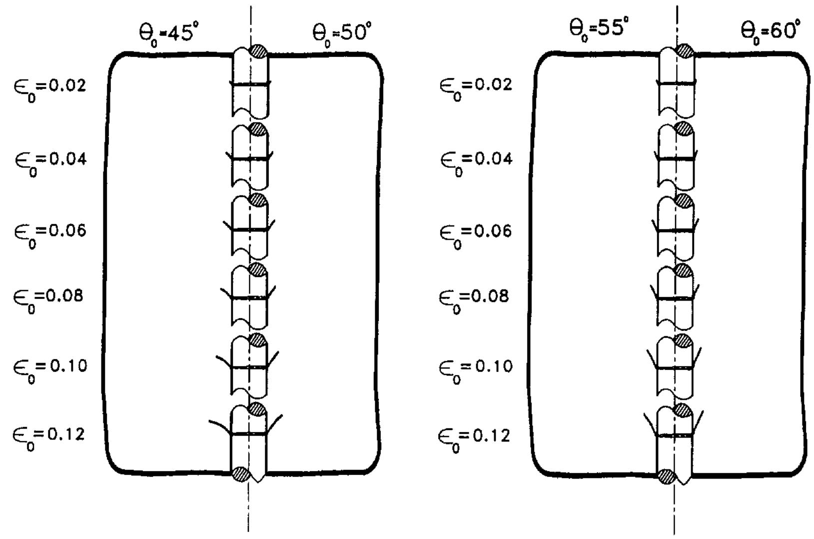

Fig. 6 Matrix crack extension at a cracked fiber location: elemental conical crack oriented at an arbitrary inclination to the fiber

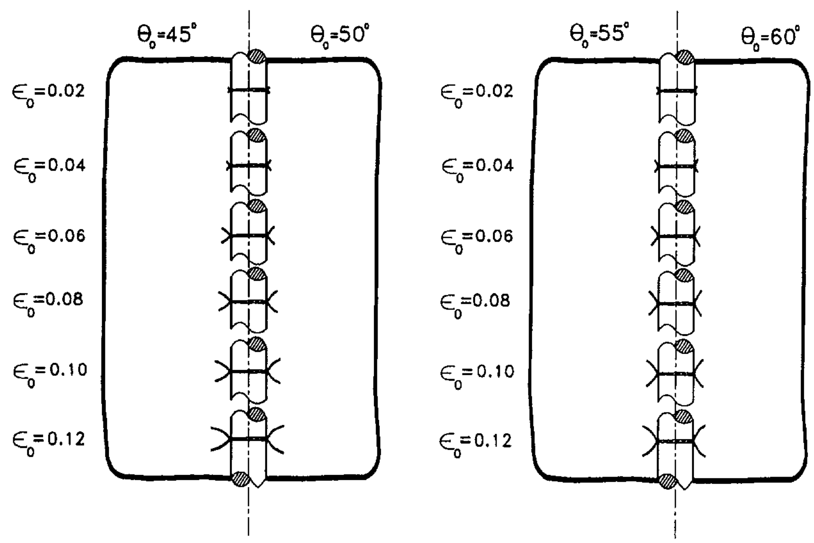

Fig. 7 Matrix crack extension at a cracked fiber location: elemental conical cracks symmetrically placed about the plane of crack fiber

location. In the numerical computations, the criteria for crack extension is checked at both crack-tip locations and the crack extension is allowed to take place at the appropriate location which satisfies the crack extension criterion. Figure 8 illustrates the crack extension patterns derived for initial conical crack orientations in the range $\theta_0 \in$ (45 deg, 60 deg). Figure 8 also illustrates the extent of crack extension either at the tip of the conical crack or at the penny-shaped crack consistent with the level of axial strain in the composite region. The results of additional computations indicate that for θ_0 within the range (0, 45 deg), the conical starter cracks essentially remain dormant and the crack extension mainly occurs at the location of the penny-shaped crack. For $\theta_0 = 60$ deg and 70 deg, crack extension can occur at both crack-tip locations. When $\theta_0 = 75$ deg, the conical crack extension mode dominates initially, and the tip of crack extension must be remote from the fiber to initiate the extension of the penny-shaped crack. Figure 9 illustrates the matrix crack extension characteristics for the situation where the penny-shaped crack at the cracked fiber location interacts with conical starter cracks which are symmetrically inclined to the axis of the fiber. Here again, computations carried out indicate that the conical starter crack does not extend at values of $\theta_0 < 30$ deg. With increasing θ_0 (e.g., $\theta_0 = 45$ deg), the conical starter crack will extend but such crack extensions will take place only as the penny-shaped crack extends to regions remote from the cracked fiber locations. For the larger values of θ_0, crack extension takes place mainly within the conical crack tip. The results are presented for various values of the applied strain ϵ_0. It is also evident that the extent of crack extension can be influenced by the symmetry or asymmetry in the orientation of the conical starter cracks.

The numerical modeling technique is now used to provide a comparison for the experimental results derived from the actual fragmentation tests. From the experimental results presented in the companion paper (Busschen and Selvadurai (1995), Table 2) it is evident that all fragmentation test specimens display a variable matrix modulus E_m. The development of numerical results for all fragmentation test specimens 1 to 5 will involve an inordinate amount of computation. For this reason, attention is focused on the two fragmentation test specimens which give the largest group of conical and combined cracks. From Table 4 of Busschen and Selvadurai (1995) it is evident that test specimens 1 and 5 can be used as typical experimental data sets for purposes of comparison. It is also noted that in these specimens the

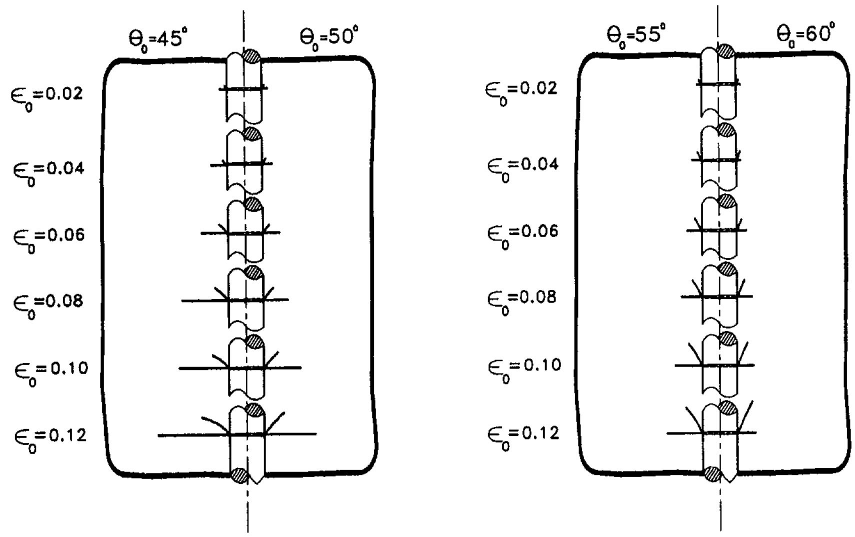

Fig. 8 Matrix crack extension at a cracked fiber location: a combination of an elemental penny-shaped crack and an elemental conical crack

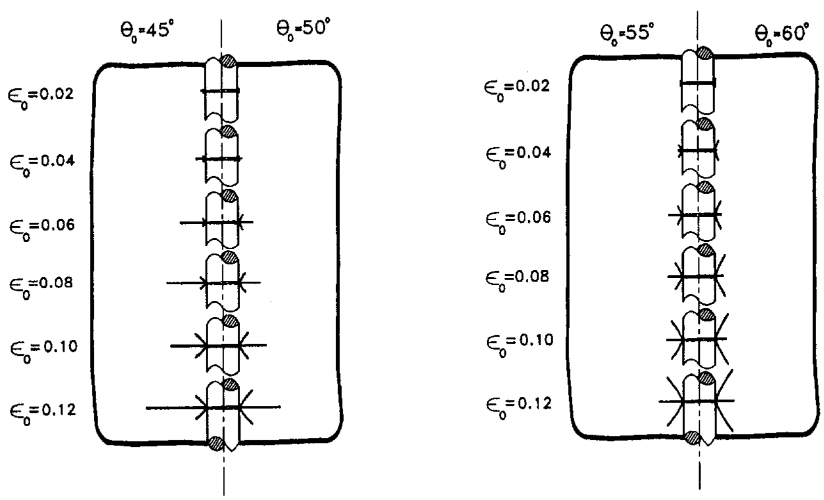

Fig. 9 Matrix crack extension at a cracked fiber location: a combination of an elemental penny-shaped crack and symmetrically placed elemental conical cracks

orientations of the initial starter crack have been accurately determined. The elastic properties of the polyester matrix used in these specimens are given in Table 2 of the companion article. The boundary element method and the fracture mechanics computations are used to compute the crack extension paths for both symmetrically placed single conical cracks and symmetrically placed single conical cracks interacting with a penny-shaped crack. Figure 10 presents the results of the comparison derived for the cases of the symmetrically placed conical cracks with $\theta_0 = 39$ deg and $\theta_0 = 45$ deg. The result for $\theta_0 = 45$ deg is provided only for purposes of comparison. The experimental results derived via the image analysis technique are classified as the *accurate mean contour*. The extended path of the cracks are derived for a strain level of $\epsilon_0 = 0.043$. Figure 11 presents the comparison between the computations for $\theta_0 = 39$ deg and $\theta_0 = 45$ deg and analogous results derived via the experimental data set which is classified as the *approximate mean contour*. It is clearly evident that the general trends indicated in the computations compare well with experimental data. We now focus on the comparison of results derived for the situation where the symmetrically placed conical crack interacts with a penny-shaped crack during the simultaneous crack extension process. In this case the initial inclination of the conical crack is assumed to be $\theta_0 = 34$ deg and the applied maximum strain $\epsilon_0 = 0.108$. Figure 12 illustrates the limits of crack extension derived via the computational scheme and the set of experimental data identified as the *accurate mean contour*. The result for $\theta_0 = 45$ deg is again presented for purposes of comparison. Analogous comparisons of computational results and the data identified with the approximate mean contour are presented in Fig. 13. In these representations the experimental results for the penny-shaped crack record either accurate or approximate contours. As is evident, these contour bounds for the penny-shaped crack indicate trends consistent with experimental data. A further comparison can be made by examining the values of c (radius of purely conical crack), c_1 (radius of the conical crack part of combined crack), and c_2 (radius of the penny-shaped crack) obtained at the limit of the axial strain $\epsilon_0 = 0.108$. The comparisons are given in Table 1. Further comparisons can be also made by using the results for the computational modeling given in Table 1 with the experimental results for specimens 2, 3, and 4 given in Table 4 of Busschen and Selvadurai (1995).

Conclusions

The integrity of bond between a reinforcing fiber and the surrounding matrix is an important property of a fiber-reinforced composite material. As the bond strength is enhanced

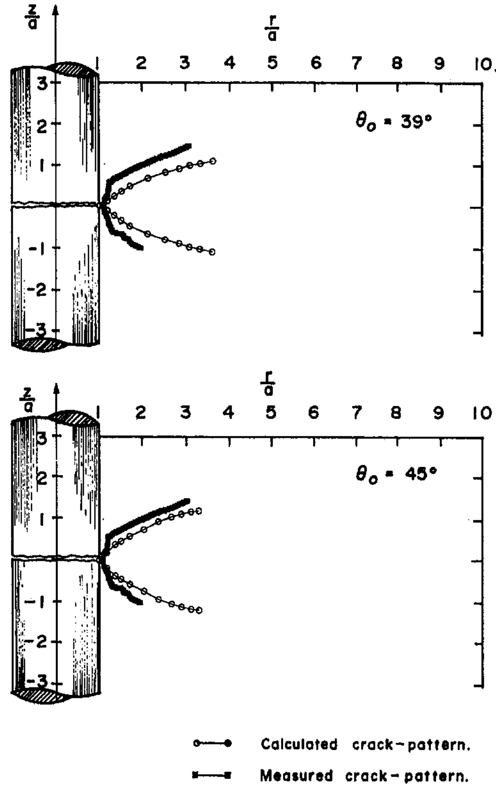

Fig. 10 Matrix crack extension due to the growth of conoidal cracks: a comparison of experimental results and computational estimates (accurate experimental data)

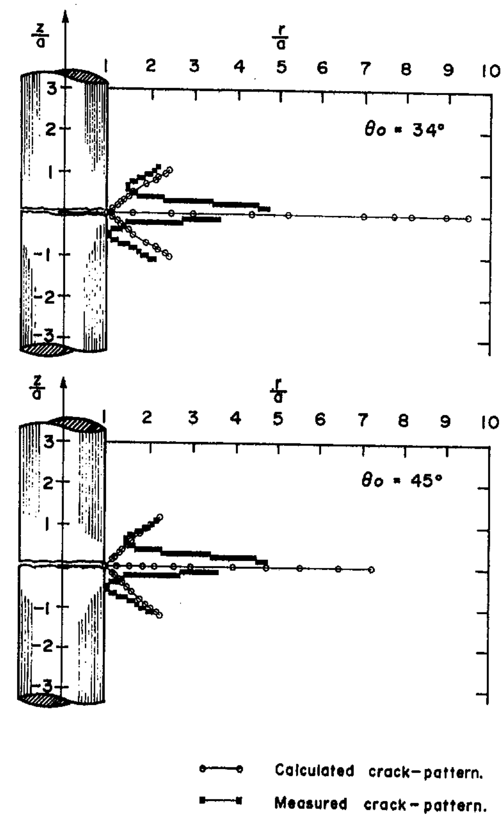

Fig. 12 Matrix crack extension due to the simultaneous growth of conoidal and penny-shaped cracks: a comparison of experimental results and computational estimates (accurate experimental data)

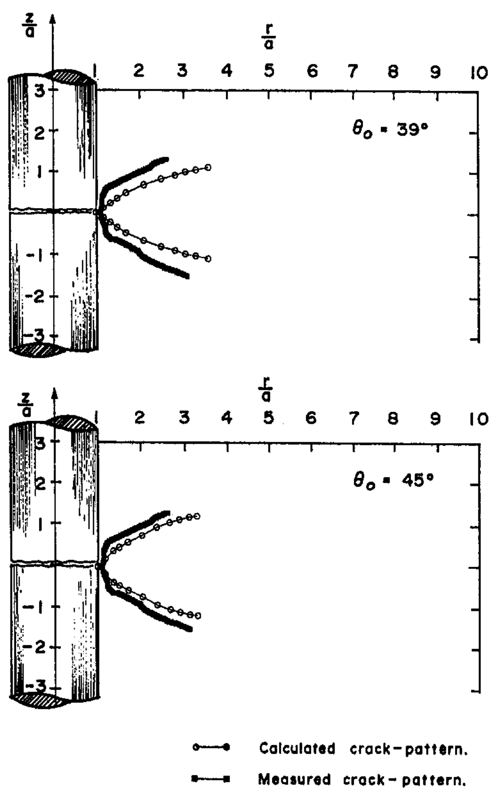

Fig. 11 Matrix crack extension due to the growth of conoidal cracks: a comparison of experimental results and computational estimates (approximate experimental data)

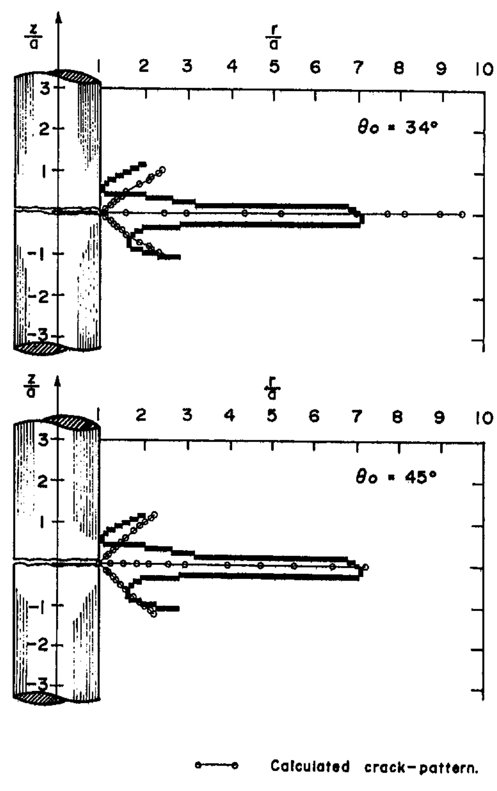

Fig. 13 Matrix crack extension due to the simultaneous growth of conoidal and penny-shaped cracks: a comparison of experimental results and computational estimates (approximate experimental data)

Table 1 Comparison of computational estimates and experimental data

	Specimen 1			Specimen 5		
	c/a	c_1/a	c_2/a	c/a	c_1/a	c_2/a
Theory	3.65	2.38	9.01	3.65	2.38	9.01
$(\text{Experiment})_{\text{Accurate}}$	2.53	1.69	2.84*	2.96	2.17	4.79
$(\text{Experiment})_{\text{Approximate}}$	2.91	2.42	3.36*	3.18	2.44	7.20

[* In these cases the boundary of the penny-shaped crack is not completely defined.]

by the use of coupling agents the role of matrix fracture has an important influence in determining the transverse strength of unidirectional fiber-reinforced composites. The fragmentation test is an effective method for the observation of fracture processes in the matrix in the presence of strong interface adhesion. This test is considered to be a more realistic analogue, in contrast to the testing of the matrix alone, for the investigation of matrix fracture in the vicinity of a fiber fracture. The objective of this phase of the research program is to provide a suitable computational procedure which can adequately model the developing matrix cracking in the fragmentation test. The modeling of fracture processes in predominantly brittle elastic materials such as brittle matrices in composites, ceramics, concrete, rock, etc., is a difficult exercise in computational mechanics. The crack extension is invariably a dynamic process. In the fragmentation test, however, the stable growth of matrix cracking can be exercised by suitable controlled straining of the active section of the fragmentation test specimen. Consequently, the mechanics of crack extension can be examined by appeal to quasi-static computational modeling. In such an exercise, the growth of matrix cracking at a cracked fiber location is assumed to occur by the extension of a nucleated or starter crack, which extends to the matrix region. In general, these starter cracks could have arbitrary three-dimensional configurations; for the purposes of the analyses it is assumed that the nucleated cracks can be composed of either individual or combined arrangements of conical and penny-shaped cracks. An alternative to the nucleated crack concept is to postulate a criterion, which could initiate cracking into the matrix region commencing at the boundary of a cracked fiber. Such an analysis is a complex exercise in fracture mechanics involving crack initiation at a bimaterial corner region. In addition to the assumption of a nucleated starter crack, it is necessary to specify criteria for the onset of crack extension and for the orientation of crack growth. In this study two relatively simple forms of these criteria are adopted for the computational modeling of crack extension.

The methodologies discussed here are implemented in a boundary element model which examines the quasi-static growth of a variety of configurations of starter cracks with conical and/or penny-shaped forms.

It is shown that the *boundary element based* computational scheme can be successfully employed to examine the matrix crack growth with conoidal and penny-shaped topographies. The boundary element scheme is particularly efficient for the study of crack extension in brittle solids since the incremental growth of the crack can be accommodated very conveniently. This is in contrast to other numerical schemes such as finite element schemes where constant remeshing at the crack-tip location is necessary to accommodate crack growth processes without specified orientations for the growth direction.

Finally, the computational procedure is employed to predict the growth of matrix cracking at a cracked fiber location. The correlations are established for conical cracks which have been measured accurately in the experimental research program. In order to establish the correlation it is necessary to specify the orientation of the conical crack, with respect to the fiber axis, as determined in the experiments. The specification of the orientation of the conical starter crack can certainly be regarded as a limitation of the modeling exercise. It is foreseeable certain additional criteria may need to be invoked to determine precisely the orientation of such conical matrix cracks which can initiate at the inception (dynamic fracture) of an embedded fiber. Similar uncertainties are encountered in the consideration of fracture initiation due to indentation where the elasticity mismatch between the indentor and the contacting surface and the local geometry at the contact boundary (in this case the local geometry at the fractured fiber boundary) will influence the orientation of the starter crack. It is, however, observed that when the initial conical crack orientations are specified, the crack growth paths observed in the experiments are predicted, reasonably accurately, with the computational model.

Studies in fracture mechanics of the brittle matrix phase of composite materials have important considerations in establishing the transverse strength of unidirectional fiber reinforced materials. With the availability of a computational modeling procedure it is possible to contemplate on the prediction of crack propagation within the matrix of a fiber-reinforced material in which the transverse tensile matrix fracture is governed by matrix crack extension within the random network of reinforcing fibers. The research also identifies certain fundamental issues pertaining to matrix crack initiation at cracked fiber boundaries which merit further study.

References

Atkinson, C., 1979, "Stress Singularities and Fracture Mechanics," ASME *Applied Mechanics Reviews*, Vol. 32, pp. 123–135.

Atluri, S. N., ed., 1991, *Computational Methods in Mechanics of Fracture, Vol. 2, Computational Methods in Mechanics*, J. D. Achenbach, ed., North-Holland, The Netherlands.

Banerjee, P. K., and Butterfield, R., 1981, *Boundary Element Methods for Engineering Science*, McGraw-Hill, New York.

Barsoum, R. S., 1976, "On the Use of Isoparametric Finite Elements in Linear Fracture Mechanics," *Int. J. Num. Meth. Engng.*, Vol. 10, pp. 25–37.

Blandford, G. E., Ingraffea, A. R., and Liggett, J. A., 1981, "Two-Dimensional Stress Intensity Factor Computations Using the Boundary Element Method," *Int. J. Num. Meth. Engng.*, Vol. 17, pp. 387–404.

Brebbia, C. A., Telles, J. C. F., and Wrobel, L. C., 1984, *Boundary Element Techniques*, Springer-Verlag, Berlin.

Brebbia, C. A., and Aliabadi, M. H., 1991, *Numerical Fracture Mechanics*, Computational Mechanics Publications, U.K.

Broek, D., 1982, *Elementary Engineering Fracture Mechanics*, Martinus Nijhoff Publ., The Hague.

Busschen, A., ten, and Selvadurai, A. P. S., 1995, "Mechanics of the Segmentation of an Embedded Fiber, Part I: Experimental Investigations," ASME JOURNAL OF APPLIED MECHANICS, Vol. 62, pp. 87–97.

Cruse, T., and Wilson, R. B., 1977, "Boundary Integral Equation Method for Elastic Fracture Mechanics," AFSOR-TR-78-0355, 10–11.

Cherepanov, G. P., 1979, *Mechanics of Brittle Fracture*, McGraw-Hill, New York.

Dvorak, G. J., ed., 1991, "Inelastic Deformations of Composite Materials," *Proc. IUTAM Symposium*, Springer-Verlag, Berlin.

Erdogan, F., and Sih, G. C., 1963, "On the Crack Extension of Plates Under Plane Loading and Transverse Shear," ASME *Journal of Basic Engineering*, Vol. 85, pp. 519–527.

Hashin, Z., and Herakovich, C. T., eds., 1983, "Mechanics of Composite Materials: Recent Advances," *Proceedings of the IUTAM Symposium on Mechanics of Composite Materials*, Pergamon Press, New York.

Hellan, K., 1985, *Introduction to Fracture Mechanics*, McGraw-Hill, New York.

Henshell, R. D., and Shaw, K. G., 1975, "Crack Tip Finite Elements are Unnecessary," *Int. J. Num. Math. Eng.*, Vol. 9, pp. 495–507.

Kanninen, M. F., and Popelar, C. H., 1985, *Advanced Fracture Mechanics*, Oxford University Press, Oxford, U.K.

Kassir, M. K., and Sih, G. C., 1975, *Three-Dimensional Crack Problems, Vol. 2, Mechanics of Fracture*, G. C. Sih, ed., Nordhoff Int. Publ., Leyden, The Netherlands.

Kelly, A., and Rabotnov, Yu, N., eds., 1983, *Handbook of Composites*, Vol. 1–4, North-Holland, Amsterdam, The Netherlands.

Kermanidis, Th., 1975, "Numerical Solution for Axially Symmetrical Elasticity Problems," *Int. J. Solids Struct.*, Vol. 11, pp. 495–500.

Lawn, B. R., and Wilshaw, T. R., 1975, *Fracture of Brittle Solids*, Cambridge University Press, Cambridge, U.K.

Liebowitz, H., ed., 1968, *Fracture*, Vol. I–IV, Pergamon Press, Oxford.

Piggott, M. R., 1980, *Load Bearing Fibre Composites*, Pergamon Press, New York.

Selvadurai, A. P. S., ed., 1981, *Mechanics of Structured Media, Proceedings of the Int. Symp. on the Mechanical Behaviour of Structured Media* (Studies in Applied Mechanics, Vols. 5A and 5B), Elsevier, Amsterdam, The Netherlands.

Selvadurai, A. P. S., and Au, M. C., 1988, "Cracks with Frictional Surfaces: A Boundary Element Approach," *Proceedings of the 9th Boundary Element Conference*, C. A. Brebbia, ed., Springer-Verlag, Berlin, pp. 211–230.

Selvadurai, A. P. S., and Au, M. C., 1989, "Crack Behaviour Associated with Contact Problems with Non-linear Interface Constraints," *Boundary Element Techniques: Applications in Engineering*, C. A. Brebbia and N. Zamani, eds., Proceedings of the Boundary Element Technology Conference, Windsor, Ontario, Computational Mechanics Publ., pp. 1–17.

Selvadurai, A. P. S., 1991, "Cracks at the Extremities of Cylindrical Fibre Inclusion," *Proc. IUTAM Symp. Inelastic Deformation of Composite Materials*, G. J. Dvorak, ed., Springer-Verlag, Berlin, pp. 147–171.

Shah, S. P., and Swartz, S. E., eds., 1987, *Fracture of Concrete and Rock, SEM-RILEM International Conference*, Springer-Verlag, Berlin.

Sih, G. C., 1973, "Some Basic Problems in Fracture Mechanics and New Concepts," *Journal of Engineering Fracture Mechanics*, Vol. 5, pp. 365–377.

Sih, G. C., 1974, "Strain Energy Density Factor Applied to Mixed Mode Crack Problems," *International Journal of Fracture*, Vol. 10, pp. 305–321.

Sih, G. C., 1975, "Application of the Strain Energy Density Theory to Fundamental Fracture Problems," *Recent Advances in Engineering Science*, Vol. 6, T. S. Chang, ed., Scientific Publ., Boston, pp. 221–234.

Sih, G. C., 1991, *Mechanics of Fracture Initiation and Propagation*, Kluwer Academic Publisher, Dordrecht, The Netherlands.

Sih, G. C., and Tamusz, V. P., eds., 1979, *Fracture of Composite Materials, Proceedings of the 1st USA-USSR Symposium*, Sijthoff and Noordhoff, The Netherlands.

Sih, G. C., and Theocaris, P. S., eds., 1981, *Mixed Mode Crack Propagation*, Proc. 1st U.S.-Greece Symposium, Athens, Greece, Sijthoff and Noordhoff, Alpen aan den Rijn, The Netherlands.

Smith, R. N. L., and Mason, J. C., 1982, "A Boundary Element Method for Curved Crack Problems in Two Dimensions," *Boundary Element Methods in Engineering*, C. A. Brebbia, ed., Springer-Verlag, Berlin, pp. 472–484.

Zienkiewicz, O. C., 1977, *The Finite Element Method*, McGraw-Hill, New York.